Journal of Medicinal Chemistry

ARTICLE

pubs.acs.org/jmc

Characterization of a Designed Vascular Endothelial Growth Factor Receptor Antagonist Helical Peptide with Antiangiogenic Activity in Vivo†

Anna Basile,[‡,∞] Annarita Del Gatto,[§,∞] Donatella Diana,[§] Rossella Di Stasi,[§] Antonia Falco,[‡] Michelina Festa,[‡] Alessandra Rosati,[‡] Antonio Barbieri,[∥] Renato Franco,[∥] Claudio Arra,[∥] Carlo Pedone,[⊥] Roberto Fattorusso,[#] Maria Caterina Turco,[‡] and Luca Domenico D'Andrea*[,§]

[‡]Dipartimento di Scienze Farmaceutiche, Università di Salerno and BioUniverSA SRL, Salerno, Italy

[§]Istituto di Biostrutture e Bioimmagini, CNR, Via Mezzocannone 16, 80134 Napoli, Italy

[∥]Istituto Nazionale Tumori "Fondazione G. Pascale", Napoli, Italy

[⊥]Dipartimento delle Scienze Biologiche, Università di Napoli "Federico II", Napoli, Italy

[#]Dipartimento di Scienze Ambientali, Seconda Università di Napoli, Caserta, Italy

Supporting Information

ABSTRACT: Angiogenesis is a fundamental process underlining physiological and pathological conditions. It is mainly regulated by the vascular endothelial growth factor (VEGF) and its receptors, which are the main targets of molecules able to modulate the angiogenic response. Pharmaceutical therapies based on antiangiogenic drugs represent a promising approach for the treatment of several socially important diseases. We report the biological and structural characterization of a VEGF receptor binder peptide designed on the N-terminal helix of VEGF. The reported experimental evidence shows that the peptide assumes in water a well-defined helical conformation and indicates that this peptide is a VEGF receptor antagonist and possesses antiangiogenic biological activity. In particular, it inhibits VEGF stimulated endothelial cell proliferation, activation, and survival, as well as angiogenesis and tumor progression in vivo. This peptide is a candidate for the development of novel peptide-based drugs for the treatment of diseases associated with excessive VEGF-dependent angiogenesis.

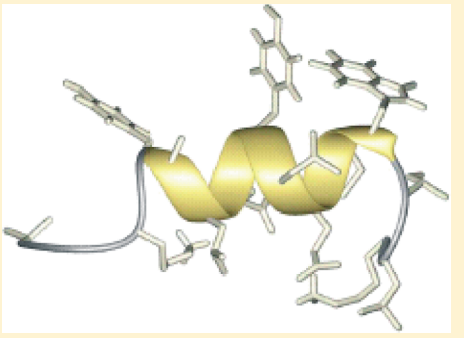

INTRODUCTION

Angiogenesis is a fundamental process for healing, reproduction, and embryonic development. It involves the growth of new blood vessels from pre-existing vessels, and it is intimately associated with endothelial cell (EC) migration and proliferation. ECs are particularly active during embryonic development, while during adult life EC's turnover is very low and limited to specific physiological processes. In a healthy individual physiological angiogenesis is regulated by fine-tuning the concentration of several pro- and antiangiogenic factors. Pathological angiogenesis occurs when, under specific stimuli such as hypoxia, the equilibrium is lost and human diseases evolve.[1] The prevalence of proangiogenic factors (excessive angiogenesis) is associated, for example, with cancer, ocular vascular diseases, rheumatoid arthritis, and psoriasis, whereas insufficient angiogenesis is at the basis of cardiovascular diseases, stroke, preeclampsia, and a reduced capacity for tissue regeneration. In this context, the ability to pharmacologically modulate the angiogenic response is a promising opportunity for therapy.[2,3]

The main regulator of physiological and pathological angiogenesis is the vascular endothelial growth factor (VEGF). It induces EC proliferation and migration, increases vascular permeability, and promotes EC survival.[4] Recently, the VEGF role in neurogenesis and neuroprotection has also been highlighted.[5] VEGF (or VEGF-A) is a homodimeric disulfide-bound glycoprotein belonging to the cystine knot growth factor family. It is encoded by a single gene that is expressed in several isoforms because of different splicing events. $VEGF_{165}$, the most abundant isoform, is a 45 KDa glycoprotein, and it binds to heparin with high affinity. The biological function of VEGF is mediated by the binding to two tyrosine kinase receptors, VEGFR1 (or Flt1) and VEGFR2 (or KDR), and neuropilin co-receptors. VEGF induces receptor dimerization that triggers kinase domain autophosphorylation and activation of intracellular pathways.[6] Both receptors are fundamental to the development of a functional vascular network during embryonic and postnatal development. During

Received: November 9, 2010
Published: January 31, 2011

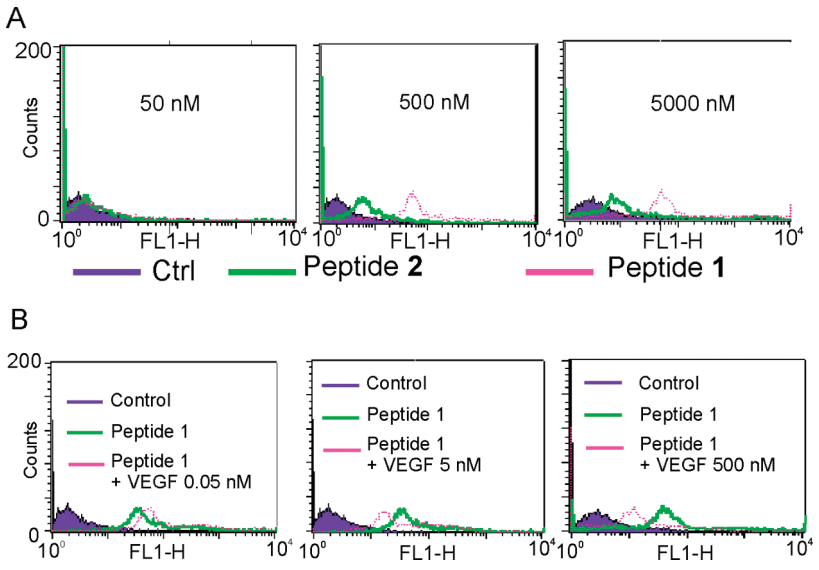

Figure 1. Receptor binding studies by flow cytometry. (A) HUVE cells (3×10^4/100 μL) were incubated with **1-Fluo** (pink curve) or **2-Fluo** (green curve) peptide at the indicated concentrations. In violet is reported the cell autofluorescence. (B) HUVE cells (3×10^4/100 μL) were incubated with peptide **1-Fluo** (500 nM) and unlabeled $VEGF_{165}$ (0.05, 5, and 500 nM) (pink curve) for 5 min at 4 °C in the dark.

the adult life, when angiogenesis is quiescent, they seem to mediate different biological functions. VEGFR2 is directly involved in EC proliferation and angiogenesis, whereas a decoy function was hypothesized for VEGFR1.[4,6] However, the VEGFR1 role in pathological angiogenesis and cross-talking between the two receptors was demonstrated.[7,8] VEGF is involved in several diseases dependent on excessive and insufficient angiogenesis,[9] making the molecular system VEGF-receptors a valuable target for therapeutic and diagnostic applications. In fact, monoclonal anti-VEGF antibodies (bevacizumab, ranibizumab), anti-VEGF aptamer (pegaptanib), and VEGFR tyrosine kinase inhibitors (sorafenib and sunitinib) were approved as drugs for antiangiogenic therapy to treat cancer and age related macular diseases.

In the present paper we report the structural and biological characterization of a 15-mer peptide (**1**), which reproduces the VEGF N-terminal helix. This peptide assumes in water a well-defined helical conformation, binds to VEGF receptors, and inhibits the VEGF biological activity. Moreover, in vivo experiments showed the ability of this molecule to inhibit VEGF-induced capillary formation and tumor growth. Peptide **1** is a promising candidate for the treatment of diseases associated with excessive VEGF-dependent angiogenesis.

RESULTS

Molecular Design. The peptide design was conducted as described by D'Andrea et al.[10] Briefly, on the basis of the X-ray structure of the VEGF/VEGFR1 domain 2 complex,[11] we designed a peptide reproducing the VEGF N-terminal helix (residues 17−25) and containing five (Phe17, Met18, Tyr21, Gln22, and Tyr25) out of 21 residues situated at less than 4.5 Å from the receptor (peptide **1** residues: Trp4, Met5, Tyr8, Gln9, and Tyr12). The peptide helix conformation was stabilized by introducing N- and C-capping sequences (Leu2/Thr3 and Lys13/Gly14/Ile15, respectively), amino acids with intrinsic helix propensity (Leu7, Leu10, Ala11), and favorable electrostatic interactions. VEGF residue Phe17 was replaced in peptide **1** by Trp4 to introduce a spectroscopic probe and to increase the hydrophobic interactions with the receptors. The peptide was acetylated and amidated to avoid electrostatic repulsion between peptide terminal charges and helix dipoles.

Binding Analysis of Peptide 1 to HUVE Cells. To verify the receptors binding properties of peptide **1**, HUVE cells were incubated for 5 min at 4 °C in the dark with increasing concentrations (50, 500, and 5000 nM) of fluorescein-conjugated peptide **1** (**1-Fluo**) or scrambled peptide **2** (**2-Fluo**) and analyzed by flow cytometry. As shown in Figure 1A, cells incubated with peptide **1-Fluo** (pink curve) showed a considerable fluorescence intensity with respect to the untreated cells (violet curve) and the scrambled peptide **2-Fluo** (green curve), suggesting a specific binding of peptide **1** to the cell membranes. Next, we verified if peptide binding was mediated by VEGF receptors (Figure 1B). HUVECs were incubated with a fixed concentration (500 nM) of peptide **1-Fluo** and increasing amounts of human recombinant VEGF (from 0.05 to 500 nM). Flow cytometry analysis displayed a significant reduction in peptide **1-Fluo** fluorescent signal (226.95 ± 7.99) when VEGF was added to the reaction mix (pink curve) at 5 nM (93.05 ± 3.60) and 500 nM (50.05 ± 5.02). As a control of specific binding of peptide **1-Fluo** and VEGF to VEGF receptors, a phycoerythrin (PE) conjugated-β-1 integrin antibody was used. Cells treated with anti-PE-β-1 integrin showed a high intensity of fluorescence due to interaction with integrin receptors located on the cell membrane. No variation of fluorescence intensity was observed when VEGF (500 nM) was added, because of its failure to interact with integrins (data not shown). These results indicate that peptide **1** binds to endothelial cells surface and competes with VEGF for a binding site on endothelial cell membranes.

Inhibition of VEGF-Induced Intracellular Pathways by Peptide 1. The binding of VEGF to its receptors activates specific intracellular pathways in ECs which end up in cell proliferation, migration, survival, and NO production. In order to evaluate the biological properties of peptide **1**, we analyzed the activation state of key intracellular enzymes on VEGF signaling

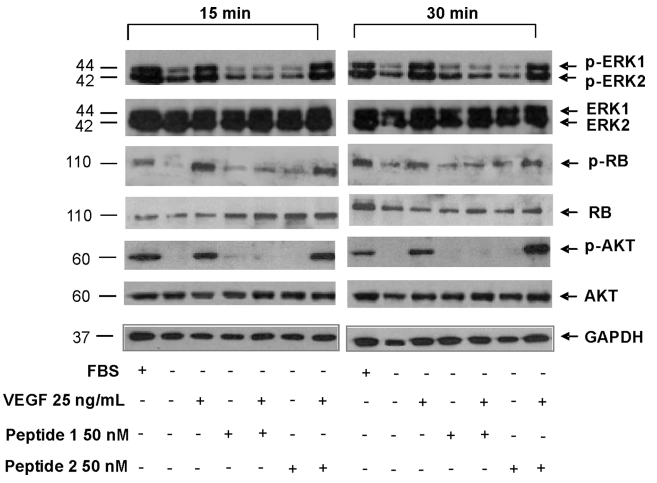

Figure 2. VEGF-dependent intracellular pathway analyses. HUVE cells were incubated for 15 and 30 min at 37 °C in starvation medium (EBM-2, 0,1% heparin, 0,1% BSA) with **1** or **2** (50 nM) peptide in the presence or absence of VEGF. Total protein extracted from cells were analyzed by Western blot using anti-phospho ERK1/2, anti-phospho AKT, and anti-phospho RB. Anti-ERK1/2, anti-AKT, anti-RB, and anti-GAPDH antibodies were used as loading control.

cascade when cells were incubated with peptide **1** in the presence or absence of VEGF.

It is well established that VEGF binding to HUVECs induces the activation of ERK and AKT kinases,[12,13] resulting in cell proliferation and inhibition of cell apoptosis. We therefore investigated whether peptide **1** binding to VEGF receptors on ECs modulates ERK1/2 and AKT activation (Figure 2). Serum deprived HUVECs were treated for 15 and 30 min with **1** and **2** (50 nM) peptides in the presence or absence of VEGF (25 ng/mL). Western blot analysis of VEGF-stimulated cell lysates displayed appreciable levels of the phosphorylated (activated) ERK1/2 kinase and AKT. These levels were highly reduced in cells incubated with VEGF in the presence of peptide **1** but not in presence of peptide **2**. Peptide **1** alone was ineffective to elicit any biological response. These experiments suggest that peptide **1** is a VEGF receptor antagonist and is able to interfere with the activation of intracellular VEGF-dependent pathways. As consequence, peptide **1** should be able to inhibit the associated cellular events such as ECs survival and proliferation.

Inhibition of VEGF Survival Activity. To investigate whether the designed peptide was able to compete with VEGF antiapoptotic activity, we analyzed the activation of caspase-3 in serum-deprived human primary endothelial cells. While >60 U/mL of activated caspase-3 was evidenced in cell lysates from FBS-deprived cells, cells from cultures with VEGF appeared to contain <30 U/mL of the enzyme activity. Therefore, the addition of VEGF partially rescued, as expected,[14] HUVECs from apoptosis. Serum deprived HUVECs were incubated with peptide **1** (12.5 and 50 nM) or peptide **2** (50 nM) in the presence or absence of VEGF (25 ng/mL). Caspase-3 activity in presence of VEGF, measured after 8 h, significantly increased using peptide **1** at both 12.5 and 50 nM with respect to cells treated with both the scrambled peptide **2** and VEGF (Figure 3A). In Figure 3B, the caspase-3 activity data are reported as the percentage of rescue from caspase-3 activation with respect to cells cultured in serum deprivation medium. In the same conditions, after 24 h of treatment, apoptosis was also analyzed by

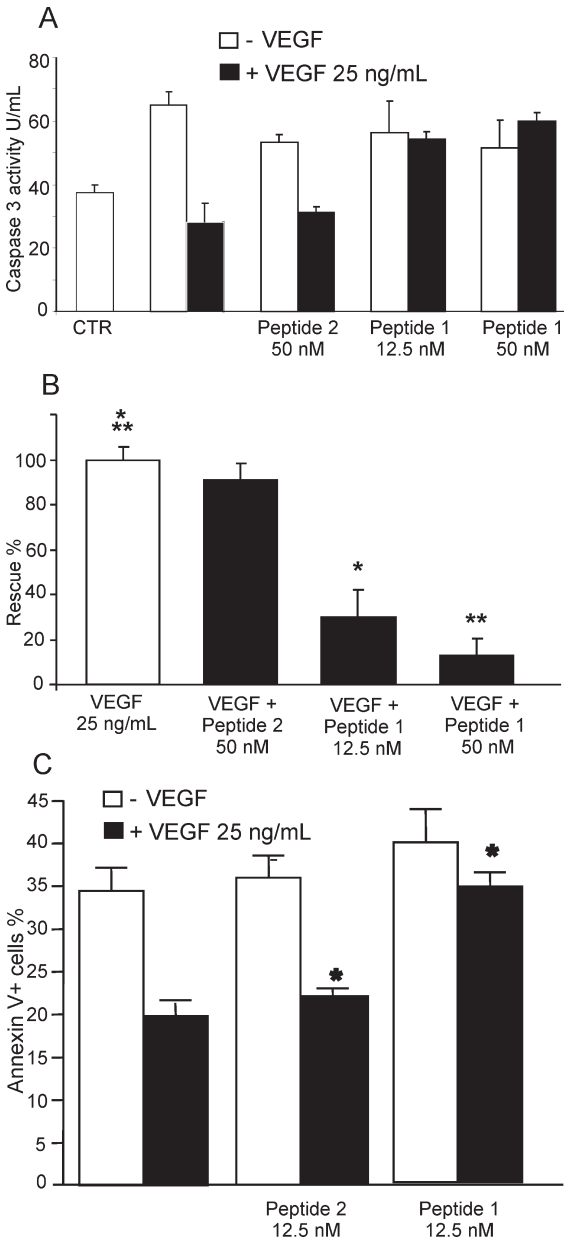

Figure 3. Effect of peptide **1** on EC survival. HUVE cells (1×10^4/cm^2) were incubated in starvation medium (EBM-2, 0,1% heparin, 0,1% BSA) with **1** or **2** peptide in the presence or absence of $VEGF_{165}$ (25 ng/mL). After 8 h, caspase-3 activity was determined. (A) Caspase-3 activity was expressed as U/mL (mean values of triplicates). (B) Percent of cell rescue from caspase-3 activation with respect to control (cells in serum starvation): *, $p = 0.015$; **, $p = 0.003$. (C) Percent of ECs positive to annexin V/FITC after 24 h: *, $p < 0.0027$. The binding was analyzed by flow cytometry.

evaluating the amount of annexin V/fluorescein isothiocyanate binding followed by flow cytometry analysis.[15] HUVECs deprived of FBS for 24 h displayed the 35% of annexin V+ cells. Such percentage was >40% reduced in cultures with 25 ng/mL VEGF. In cells cultured with VEGF and peptide **1** (12.5 nM), we found a large increase of annexin V+ cells (Figure 3C), indicating that peptide **1**, but not peptide **2**, significantly ($p < 0.02$) inhibited the antiapoptotic affect of the growth factor.

dx.doi.org/10.1021/jm101435r |J. Med. Chem. 2011, 54, 1391–1400

These data suggest an inhibitory activity of peptide **1** with respect to VEGF prosurvival effects on endothelial cells. The scrambled peptide was ineffective at the tested concentration.

Effect of Peptide 1 on Cell Proliferation. To evaluate whether the inhibition of ERK1/2 activity by peptide **1** results also in a reduced cell growth, a proliferation assay was performed on HUVECs treated, in serum deprivation conditions, with VEGF, **1** (12.5 and 50 nM), or **2** (50 nM) peptides. After 24 and 48 h of treatment cell proliferation was measured by CyQUANT NF cell proliferation assay kit. A remarkable inhibition of VEGF-induced cell proliferation was obtained in the presence of peptide **1**. In fact, after 24 h VEGF increased cellular proliferation by 58% with respect to untreated cells whereas cells incubation with peptide **1** (12.5 and 50 nM) in the presence of VEGF showed a significant reduction in cellular proliferation of about 40−45% with respect to treated cells with peptide **2** (p = 0.008) (Figure 4A). After 48 h, VEGF treatment increased cellular proliferation of 95% with respect to untreated cells whereas peptide **1** treatment (12.5 and 50 nM) in the presence of VEGF decreased cellular proliferation by more than 85−87% compared to treated cells with scrambled peptide **2** (p = 0.0001) (Figure 4B). Moreover, Western blot analysis, from whole cells proteins obtained after 24 h of treatment, confirmed ERK1/2 inactivation and reduction of phospho-RB content in cells treated with peptide **1** in the presence of VEGF (Figure 4C). Notably, the stimulatory effect of 25 ng/mL VEGF on HUVECs is completely abolished by peptide **1** even at 25 ng/mL (12.5 nM).

Antiangiogenic Activity of Peptide 1 in Vivo. We checked whether the peptide inhibited capillary formation, using an in vivo angiogenesis assay. Angioreactors filled with a solutions containing VEGF alone and in combination with peptide **1** (200 nM) and peptide **2** (200 nM) were implanted into the dorsal flank of nude mice. Endothelial cell invasion was quantified by determining the number of FITC-positive cells observed by fluorescence microscopy (Figure 5), and 20 fields for sample were analyzed. Capillary formation was extensively found in angioreactors containing VEGF alone or in combination with peptide **2**. Instead, in the presence of peptide **1** the stimulatory effect of VEGF is completely abolished. In fact, peptide **1** is able to decrease the number of endothelial cells about 85% with respect to VEGF containing angioreactors. Peptide **2** was ineffective at the tested concentration. Comparing the number of endothelial cells in angioreactors containing VEGF and peptide **1** or peptide **2**, we found that peptide **1** induces a reduction of about 85% with respect to control peptide **2**. VEGF is a potent angiogenic factor in vivo, which induces cell proliferation and migration through an extracellular matrix to form threadlike structures that join to create a network of tubules.[16,17] It is evident from the biological characterization that peptide **1** is able to inhibit the VEGF activity and shows antiangiogenic activity.

Peptide 1 Inhibits Tumor Progression in an Experimental Model of Melanoma. The ability of peptide **1** to block tumor growth was evaluated in an experimental model of melanoma. A375 cells were implanted in nude mice, and the xenografts were treated with peptide **1** or **2** (200 nM). After 15 days of treatment mice treated with intratumoral injection of peptide **1** showed a reduced tumor growth of about 36% and 47% compared to untreated (p = 0.02) and **2** treated (p = 0.01) mice, respectively (Figure 6A). The control peptide **2** was ineffective in inhibiting the tumor progression. Moreover, immunohistochemical analysis of CD31 antigen expression in tumors treated for 1 week

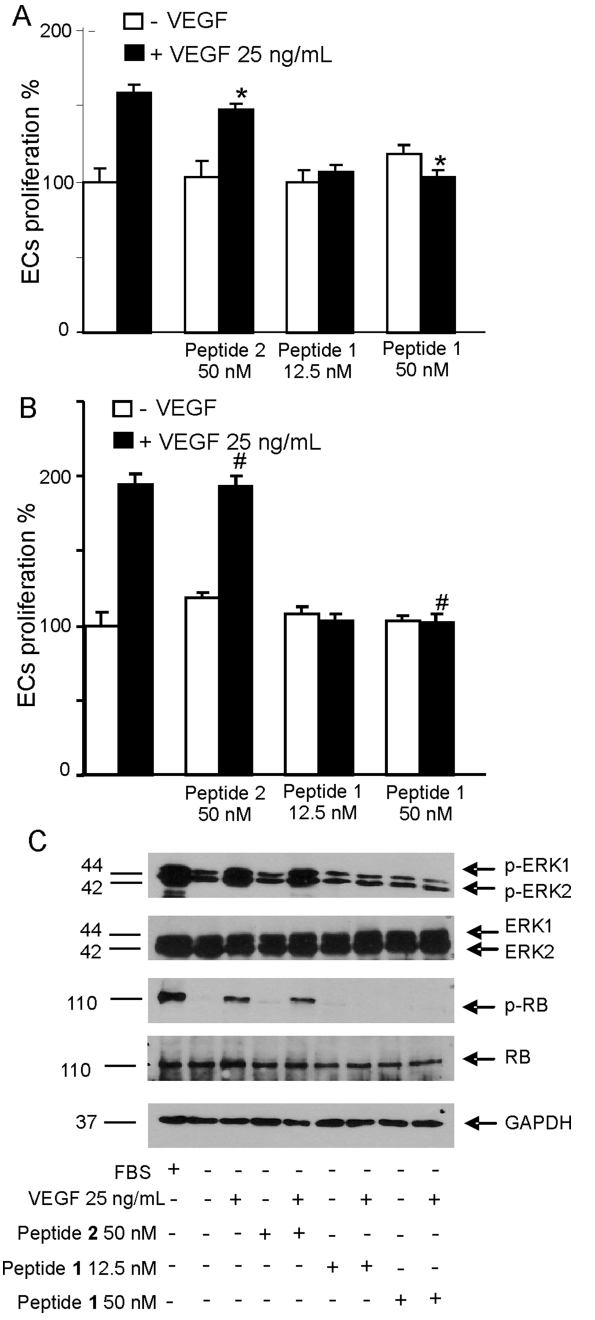

Figure 4. Effect of peptide **1** on EC proliferation. HUVE cells were incubated for 24 and 48 h at 37 °C in starvation medium (EBM-2, 0.1% heparin, 0.1% BSA) with **1** or **2** peptide at the indicated concentrations in the presence or absence of $VEGF_{165}$ (25 ng/mL). Cells were then incubated with CyQUANT NF reagent, and fluorescence intensities of quadruplicate samples were measured with a fluorescence microplate reader using excitation at 485 nm and fluorescence detection at 530 nm. Values are calculated as percentage of proliferating cells. (A) HUVEC proliferation after 24 h (∗, p = 0.008) and (B) after 48 h (#, p = 0.0001). (C) ERK1/2 phosphorylation and phospho-RB were evaluated at 24 h after incubation with **1** or **2** peptide in the presence or absence of $VEGF_{165}$ (25 ng/mL). Total protein extracted from cells was analyzed by Western blot using anti-phospho ERK1/2 and anti-phospho RB. Anti-ERK1/2, anti-RB, and anti-GAPDH antibodies were used as loading control.

with peptide **1** showed a 50% reduction of blood vessels with respect to control (p = 0.005) or peptide **2** (p = 0.004) treated

dx.doi.org/10.1021/jm101435r |J. Med. Chem. 2011, 54, 1391–1400

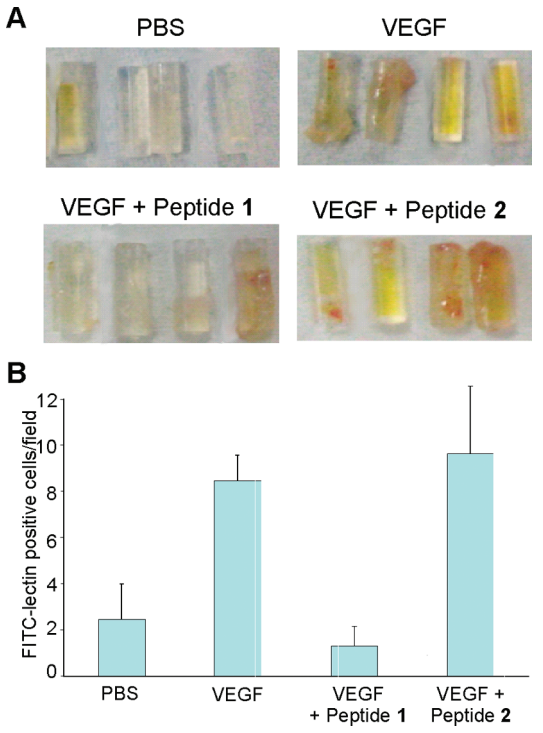

Figure 5. In vivo evaluation of the antiangiogenic activity of peptide **1**. (A) Pictures of selected implanted angioreactors after 21 days. In VEGF and VEGF/peptide **2** containing angioreactors, new vessel formation was observed. No vessel formation was observed in angioreactors containing VEGF/peptide **1**. (B) Endothelial cell population was quantified by fluorescence microscope by determining the number of FITC-lectin positive cells. Twenty fields for sample were analyzed, and results are expressed in number of FITC-lectin positive cells/field (∗, p = 0.0003; ∗∗, p = 0.000 005).

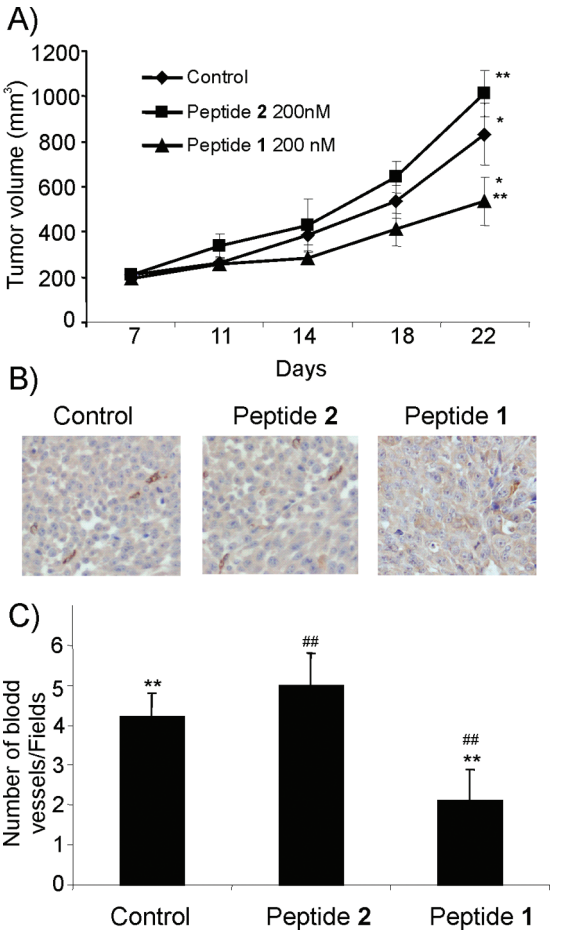

Figure 6. Effect of peptide **1** on melanoma xenograft. A375 cells (5×10^6) were injected subcutaneously onto the back of 6-week-old female athymic nude-Foxn1$^{nu/nu}$ mice. One week later, animals were randomized into three groups (10 animals per group), and control PBS and peptide **1** or **2** (200 nM) were injected in the tumors twice a week. (A) Tumor sizes in peptide **1** or **2** treated or untreated remaining mice (8 per group) were measured twice a week using a caliper (∗, p = 0.02; ∗∗, p = 0.01). (B) After 7 days of treatments, two tumors per animal group were excised and blood vessels were analyzed by immunohistochemistry with anti-CD31 rat monoclonal antibody. (C) Microvessel density in A375 xenograft was expressed as number of blood vessels/field; 10 fields for sample were analyzed (∗∗, p = 0.005; ##, p = 0.004).

mice (Figure 6B,C), indicating that peptide **1** inhibited tumor angiogenesis.

Circular Dichroism Spectroscopy. A conformational characterization in solution of peptide **1** was performed by circular dichroism spectroscopy. CD spectra of peptide **1** were recorded at pH 7.1 in 10 mM phosphate buffer at 60 μM (Supporting Information Figure S1). The analysis of the spectra indicates that peptide **1** assumes in water a predominantly helical conformation, as assessed by the presence of two minima around 208 and 222 nm.

NMR Conformational Analysis. The aggregation state of peptide **1** was determined via DOSY experiments performed under conditions identical to those used for the NMR spectroscopy structure determination. DOSY measurements at 298 K (Figure S2) provided a diffusion coefficient value of 1.91×10^{-10} $m^2 s^{-1}$, which corresponds to what is expected for a monomeric 15-mer helical peptide[18−20] in the same conditions.

A virtually complete proton assignment of the peptide (Table S1) was accomplished by a careful inspection of homonuclear 2D TOCSY, 2D NOESY, and DQF-COSY spectra, following the well established procedures of Wüthrich and co-workers.[21] The Hα chemical shift analysis, performed using the chemical shift index,[22] indicated the presence of a helical structure encompassing the central region of peptide **1** (Figure S3). A dense grouping of short- and medium-range NOEs, H_N-H_N $(i, i+1)$, $H_\alpha-H_N$ $(i, i+3)$ and $H_\alpha-H_\beta$ $(i, i+3)$ supports the presence of helical structure in this region (Figure S4). In total, 272 NOE cross peaks were assigned and integrated. Stereospecific assignment for Trp4 H_β protons was derived from the input data using the software CYANA. Moreover, 13 $^3J_{HNH\alpha}$ coupling constants were extracted from the DQF-COSY spectrum. Temperature coefficients of the amide protons of peptide **1** were also measured and indicated that the backbone amide protons of residues 3, 6, 11 could be involved in hydrogen bonding and used as constraints during structure calculations. The final input file for the CYANA structure calculation software contained 219 meaningful distance constraints (74 intraresidue, 88 short- and 57 medium-range) and 62 angle constraints which were derived from intraresidue and sequential NOEs and the $^3J_{HNH\alpha}$ coupling constants. NMR structural statistics and peptide **1** structures are shown in Table 1 and in Figure 7A, after superimposing the backbone atoms. The rms deviation values of the backbone and of the all heavy atoms of the 4−12 region are 0.22 and 0.99 Å, respectively. The Ramachandran plot of all 20 refined structures indicated that

Table 1. NMR Structural Statistics of Peptide 1

parameter	value
NOE upper distance limit	219
intraresidue	74
short distance	88
medium/long distance	57
number of dihedral angle constraints	62
residual target function, Å	0.13 ± 0.02
residual NOE violations	
number >0.1 Å	±1
maximum, Å	0.15 ± 0.02
residual angle violations	
number >2.0°	0 ± 0
maximum, Å	0
Amber energies, kJ/mol	
total	−359 ± 15
van der Waals	−126 ± 15
electrostatic	−222 ± 20
rmsd to the mean coordinates, Å	
N, Cα, C′ (3−12)	0.22 ± 0.02
all heavy atoms (3−12)	0.99 ± 0.02

the backbone dihedral angles consistently lie in the α-region. Peptide **1** adopts a well-defined helical structure encompassing the Trp4-Tyr12 region with more disordered N- and particularly C-terminus.

Serum Stability Assay. The stability of peptides **1** and **2** in 25% human serum was evaluated by HPLC. Peptides were incubated up to 24 h and aliquots taken at different times (Figure S5). Peptide **2** is almost immediately degraded showing a half-life of less than 15 min. Peptide **1** is more resistant to serum degradation with a half-life of about 90 min. After 2 h almost 40% of peptide **1** is still remaining in the serum. This amount reduced to the 10% after 24 h of incubation (data not shown). The higher stability of peptide **1** with respect to peptide **2** may be attributed to peptide **1** structural stabilization, considering that the two peptides share the same amino acid content.

DISCUSSION

Compounds targeting VEGF receptors are attractive molecules, as they have several pharmaceutical and diagnostic applications. In fact, VEGF receptor antagonists are useful for treating pharmacologically pathologies depending on excessive angiogenesis. Moreover, molecules targeting VEGF receptors are required in molecular imaging to visualize in vivo VEGF receptor expression. Peptides have been widely employed to modulate the angiogenesis, and several molecules targeting VEGF[23] and VEGF receptors[24] have been described so far. Structure-based design of VEGFR antagonists, such as peptide **1**, has been sparsely reported.[25−28] In fact, peptides targeting the extracellular domain of VEGFRs have been mainly developed using combinatorial approaches.[23,24]

In this paper we describe the biological and structural characterization of a VEGF receptor binder peptide, designed on the N-terminal helix of VEGF (residues 17−25). The experimental evidence reported shows that the peptide assumes in water a well-defined helical conformation, according to the molecular design, and indicates that peptide **1** is a VEGF receptor antagonist with an antiangiogenic biological activity. Peptide **1** helical

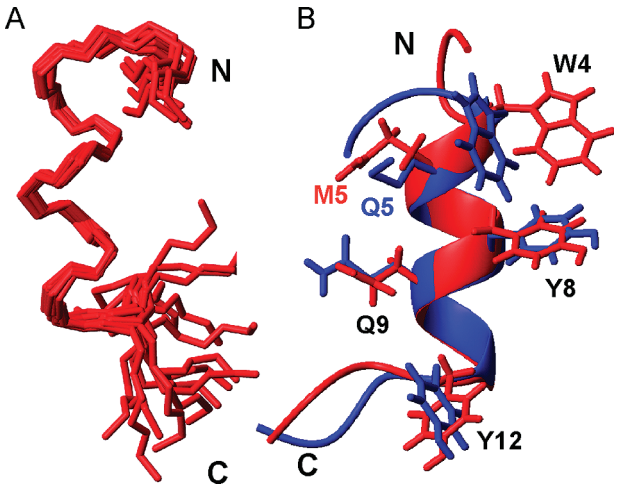

Figure 7. NMR structure of peptide **1**: (A) superposition of the backbone of the best 20 CYANA peptide **1** structures; (B) superposition of QK (blu) and **1** (red) representative structures. The residues potentially involved in the interaction with VEGF are shown.

structure includes residues 4−12, reproducing part of the three-dimensional arrangement of VEGF binding interface to the receptors. Notably this conformational preference is absent in the peptide corresponding to the natural amino acid sequence of VEGF (residues 17−25; see VEGF15 in ref 10). Binding studies showed that the peptide interacts with receptors on endothelial cell membrane, and a VEGF competition experiment suggests that these receptors are VEGFR1 and VEGFR2. Binding of VEGF to its receptors on ECs activates specific intracellular pathways, which involve kinases such as ERKs and AKT, stimulating EC proliferation, migration, survival, and NO production. In order to evaluate the biological properties of peptide **1**, we analyzed the activation state of key intracellular enzymes on VEGF signaling cascade. These experiments showed that peptide **1** is able to inhibit the activation of ERK1/2 and AKT. Moreover, it is known that VEGF stimulates angiogenesis by inducing endothelial cell proliferation and by preventing endothelial cell death (antiapoptotic function). EC proliferation and survival have been demonstrated to be mediated by VEGFR2 through the activation of intracellular pathways involving ERK1/2 and AKT, respectively.[13,29] As a consequence, the ability of peptide **1** to inhibit the phosphorylation of these key intracellular enzymes should reflect the inhibition of the associated EC functions. In fact, peptide **1** is able to block endothelial cell proliferation and the rescue from apoptosis of serum deprived endothelial cells stimulated with VEGF. Finally, we also show that the peptide is able to exert its biological activity in vivo reducing the capillary formation in an experimental model of angiogenesis and, notably, inhibiting the growth of melanoma xenograft. The reduced tumor growth correlated with the inhibition of the tumor angiogenesis, suggesting that the antiproliferative effect of peptide **1** is related to its antiangiogenic activity.

All the data presented in this work show that peptide **1** is a bioactive peptide with antiangiogenic activity. In order to be a candidate for pharmaceutical applications, peptide **1**, which is composed of natural amino acids only, has to show reasonable in vivo stability. With the aim to evolve **1** toward peptidomimetic compounds we checked its serum stability. Peptide **1** showed a half-life of about 90 min, higher than that shown by the scrambled peptide **2**. The increased serum stability could be

ascribed to the structural preorganization of **1** which renders the peptide less susceptible to the protease attack. However, the small effect on tumor growth inhibition could be ascribed to the peptide half-life, suggesting that a protease resistant analogue could achieve a better biological effect in vivo.

Previously, we described a peptide, QK, mimicking the same VEGF region as peptide **1** showing a proangiogenic biological activity in vivo.[10,30,31] The two peptides differ only for two amino acids; peptide **1** presents Met5 and Ala11 residues instead of QK residues Gln5 and Lys11. It is noteworthy that a two amino acid change in a 15 mer VEGFR binder peptide induces different biological responses. We turned to a structural approach to verify if the two different amino acids induce a diverse peptide conformation. In general, the structural analysis confirmed the high tendency of this class of peptides to adopt a stable helical conformation in water and their potential as helical scaffold. Superposition of peptide **1** and QK representative structures (Figure 7B) indicates that the two peptides fold very similarly but nonetheless exhibit structural differences at the N-terminus, which is bent in peptide **1** and not in QK. This small difference affects the conformation and probably the orientation of the Trp4 side chain that together with Met5, Tyr8, Gln9, and Tyr12 is likely involved in the interaction with VEGF receptor. It is possible that this different peptide arrangement could effectively affect the receptor molecular recognition or receptor activation, but this hypothesis needs further computational and/or experimental confirmation. Furthermore, we can speculate that a different conformational arrangement of the bound receptor, ending up in an opposite receptor activation state, could be induced by a direct role of the two different amino acids. Previous work on erythropoietin receptor peptide ligands showed that a minimal sequence perturbation (tyrosine vs 3,5-dibromotyrosine) can turn a receptor agonist into an antagonist; X-ray structure analysis of the complex between the antagonist and the EPO receptor showed that receptor dimerization still occurs but the dimer orientation is altered.[32] Of course, other hypotheses could be formulated and at the moment cannot be excluded, for example, a diverse interaction pattern with the receptors driven by the different amino acids or the different peptide total charge. The elucidation of the mechanism of action and the receptor binding properties of the two peptides will require further investigation. Nonetheless, the different bioactivity of two members of this VEGF mimicking peptide family suggests their applications as chemical biology probes to verify whether VEGF receptors present a finer molecular plasticity than so far described.

CONCLUSION

We designed and characterized a helical peptide that binds to VEGF receptors and exhibits potent antiangiogenic properties. In particular, it inhibits endothelial cell proliferation, survival, and angiogenesis in vivo. Remarkably, peptide 1 was able to reduce tumor growth in an experimental model of melanoma inhibiting the tumor angiogenesis. This peptide is a candidate for the development of novel peptide-based drugs for therapeutic application in diseases benefiting from antiangiogenic treatment such as cancer, age-related macular disease, psoriasis, and arthritis rheumatoid and for the imaging of VEGF receptors.

EXPERIMENTAL SECTION

Peptide Synthesis Reagents. All amino acids, coupling reagents, and resin were from Novabiochem-Merck (Nottingham, U.K.). Peptide synthesis solvents *N*,*N*-dimethylformammide (DMF) and dichlromethane (DCM) were obtained respectively from Romil (Cambridge, U.K.) and Sigma-Aldrich (Milan, Italy) with the lowest water content and used without further purification. Piperidine was from Biosolve (Valkenswaard, The Netherlands) and *N*,*N*-diisopropylethylamine (DIPEA) from Romil (Cambridge, U.K.). Acetic anhydride triisopropylsilane (TIS), ethanedithiol (EDT), acetonitrile (CH_3CN), trifluoracetic acid (TFA), and 6-[fluorescein-5(6)-carboxamido]hexanoic acid were from Sigma-Aldrich (Milan, Italy), and *N*,*N*,*N*′,*N*′-tetramethyl-*O*-(7-azabenzotriazol-1-yl)uronium hexafluorophosphate (HATU) was obtained from Advanced Biotech Italia (Seveso, Italy).

Peptide Synthesis. Peptides were synthesized on solid phase by standard fluorenylmethyloxycarbonyl (Fmoc) chemistry.[33] The synthesis was carried out manually on a Rink amide MBHA resin (loading of 0.5 mmol g^{-1}, 0.2 g) and Fmoc-protected standard amino acids except for the last residue (Lys1) whose side chain was protected with the methyltrityl group (Mtt). Each synthetic cycle consisted of deprotection steps (2 × 5 min) performed with 30% piperidine in DMF, coupling reactions carried out for 45 min at room temperature using a 1 mmol of amino acid (10-fold molar excess with respect to synthesis scale), HBTU (0.98 mmol), HOBt (0.98 mmol), DIPEA (2 mmol) in DMF, and a capping step (1 × 5 min) performed with a solution of acetic anhydride (0.5 M)/HOBt (0.015 M)/DIPEA (0.125 M) in DMF.

Peptide labeling with fluorescein was carried out on solid phase after selective deprotection of methyltrityl side chain protecting group of the N-terminal Lys with a solution of TFA/TIS/DCM (1:5:94 v/v/v). The side chain amine group of lysine was reacted, after a neutralization step (DIPEA 0.5 M), with 2 equiv of 6-[fluorescein-5(6)-carboxamido]-hexanoic acid in the presence of 2 equiv of HATU and 5 equiv of DIPEA in DMF overnight at room temperature.

Peptides were cleaved off from the resins and fully deprotected using a mixture of TFA/H_2O/EDT/TIS (94:2.5:2.5:1 v/v/v/v) for 3 h at room temperature. Resin was separated by filtration, and the filtrate was precipitated with cold diethyl. The precipitate was separated by centrifugation, solubilized in water, and lyophilized.

All crude products were purified by RP-HPLC on a Shimadzu LC-8A system equipped with an UV−vis detector SPD-10A using a semipreparative Phenomenex Jupiter Proteo column (250 mm × 10 mm, 90 Å) and a linear gradient from 20% to 80% of CH_3CN (0.1% TFA) in H_2O (0.1% TFA) in 30 min at a flow rate of 5 mL/min. Peptide identification and analysis were performed on a LC−MS instrument (Thermo-Finnigan) equipped with diode array detector combined with an electrospray ion source and a quadrupole mass analyzer using a Phenomenex Jupiter Proteo column (150 mm × 4.60 mm, 90 Å) and a linear gradient from 20% to 80% of CH_3CN (0.1% TFA) in H_2O (0.1% TFA) in 30 min (method A) or from 30% to 80% of CH_3CN (0.1% TFA) in H_2O (0.1% TFA) in 30 min (method B). All peptides showed a purity above 95%, based on the chromatographic peak area revealed at 210 nm.

Peptide 1 (Acetyl-KLTWMELYQLAYKGI-amide). MS *m*/*z* calcd, 1897.0 amu; found 949.4 $[M + 2H^{2+}]$. t_R = 18.4 min (method A).

Peptide 2 (Acetyl-KQMYLELGYATIKWL-amide). MS *m*/*z* calcd, 1897.0 amu; found 949.1 $[M + 2H^{2+}]$. t_R = 17.4 min (method A).

Peptide 1-Fluo (Acetyl-K(fluorescein)LTWMELYQLAYKGI-amide). MS *m*/*z* calcd, 2368.5 amu; found 1185.5 $[M + 2H^{2+}]$. t_R = 20.8 min (method A).

Peptide 2-Fluo (Acetyl-K(fluorescein)QMYLELGYATIKWL-amide). MS *m*/*z* calcd, 2368.5 amu; found 1185.4 $[M + 2H^{2+}]$. t_R = 17.9 min (method B).

Biological Reagents. Human umbilical vein endothelial cells (HUVEC) were obtained from Promocell (Heidelberg, Germany) and cultured in EGM-2 SingleQuots from Cambrex (Carlsband, CA, U.S.). Human recombinant VEGF165 was obtained from R&D (Minneapolis, MN, U.S.). Antibodies against ERK1/2 (K-23, sc-94), GAPDH, RB, and phycoerythrin conjugated-β-1 integrin (sc-13590)

were purchased from Santa Cruz Biotechnology Inc. (Santa Cruz, CA, U.S.). Antibodies against phospho-ERK 1/2 (Thr202/Tyr204, no. 9101), phospho-Akt (Ser473, no. 9271), Akt (no. 9272), and phospho-RB (Ser780, no. 9307) were purchased from Cell Signaling Technology, Inc. (Danvers, MA, U.S.). Fluorescein isothiocyanate conjugated annexin V was obtained from Bender MedSystems GmbH (Vienna, Austria). Anti-human α-tubulin was obtained from Sigma-Aldrich (St. Louis, MO, U.S.). Enhanced chemiluminescence Western blot detection reagents were purchased from Amersham Life Sciences Inc. (Arlington Heights, IL, U.S.). Secondary antibodies were purchased from Pierce (Rockford, IL, U.S.). *N*-Acetyl-DEVD-AMC (A1086) was purchased from Sigma Aldrich, Inc. (St. Louis, MO, U.S.).

Fluorescence Binding Assay. HUVEC cells were harvested, suspended at 3×10^4/100 μL in starvation medium (EBM-2, heparin 0.1%, BSA 0.1%), and then were incubated with FITC-conjugated peptide **1-Fluo** (0.05, 500, and 5000 nM) or scrambled peptide **2-Fluo** (0.05, 500, and 5000 nM) and in the presence or absence of $VEGF_{165}$ (0.05, 5, and 500 nM) for 5 min at 4 °C in the dark. After being washed with PBS, the cells were resuspended in PBS and analyzed with a FACScan (Becton Dickinson, NJ, U.S.). As technical control, an antibody phycoerythrin conjugated-β-1 integrin (1:100) was used.

Western Blotting Analysis. Cell total protein lysates were prepared in sample buffer (2% sodium dodecyl sulfate, 10% glycerol, 2% mercaptoethanol, and 60 mM Tris-HCl, pH 6.8, in demineralized water) on ice. Lysates (25 μg) were run on 12% SDS−PAGE gels and electrophoretically transferred to nitrocellulose. Nitrocellulose blots were blocked with 5% BSA in TBS Tween-20 (TBST) buffer and incubated with primary antibody in TBST-5% BSA overnight at 4 °C. Immunoreactivity was detected by sequential incubation with horseradish peroxidase conjugated secondary antibody and enhanced chemiluminescence reagents following standard protocols (Amersham Bioscience, U.K.).

Cell Proliferation Assay. HUVECs were plated at density of 1200 cells/well in 96-well poly-D-lysine-coated microplates (Becton Dickinson, NJ, U.S.). After 24 h, cells were incubated in serum deprivation conditions (EBM-2, heparin 0.1%, BSA 0.1%) with peptide **1** (25−100 ng/mL) and in the presence or absence of $VEGF_{165}$. Peptide **2** (100 ng/mL) was used as negative controls. Cell proliferation was determined by using CyQUANT NF cell proliferation assay kit (Invitrogen, Italy) at 24 and 48 h after treatment. CyQUANT NF assay is based on cellular DNA content measurement via fluorescent dye binding. Because cellular DNA content is highly regulated, it is closely proportional to cell number. Briefly, the medium was removed and cells were incubated with CyQUANT NF reagent for 1 h at 37 °C according to the manufacturer's instructions. Plates were then analyzed by using a LS5 luminescence spectometrer microplate reader (Perkin-Elmer Instruments, Milan, Italy) using an excitation wavelength of 485 nm and emission wavelength of 520 nm.

Analysis of Caspase-3 Activity. Cells (2×10^4) were lysed in a buffer containing Hepes 50 mM, DTT 1 mM, EDTA 0.1 mM, NP-40 0.1%, CHAPS 0.1%, and protein quantization was determined. Protein aliquots (20 μg) were incubated with 20 μM peptide substrate Ac-DEVD-AMC (Pharmingen, San Diego, U.S.) at 37 °C for 3 h in the lysis buffer. Caspase-3 activity was determined in the cytosolic extracts by analyzing the release of 7-amino-4-methylcoumarin (AMC) monitored by a spectrofluorometer, with excitation wavelength of 380 nm and emission wavelength of 440 nm.[34]

In Vivo Angiogenesis Assay. In vivo angiogenesis was assayed by using directed in vivo angiogenesis assay (DIVAA) (Trevigen, Gaithersburg, U.S.). Sterile silicone cylinders closed at one end, the angioreactors, were filled with 20 μL of basement membrane extract premixed with or without angiogenesis factors (VEGF, FGF) to obtain positive or negative controls, respectively. Furthermore, peptide **1** (200 nM) or scrambled peptide **2** (200 nM) was added to angioreactors. These were incubated at 37 °C for 1 h to allow gel formation before subcutaneous implantation into the dorsal flank of CD1 mice. Animals were anesthetized before implantation with 100 mg/mL ketamine HCl and 20 mg/mL xylazine injected subcutaneously. Incisions were made on the dorsal flank (left and right) of the mouse, approximately 1 cm above the hip socket, and were closed with skin staple. Vessel formation evaluation was performed after 21 days. Matrigel was removed from angioreactors and digested in 300 μL of CellSperse solution for 1 h at 37 °C. After digestion, the incubation mix was cleared by centrifugation at 250*g*. Cell pellets were resuspended in 500 μL of DMEM 10% FBS and plated on glass slides in 24-wells plates for 16 h at 37 °C in 5% CO_2. Cells were fixed with a 3.7% formaldehyde solution for 30 min at room temperature and quenched by incubation with 0.1 mM glycine for 5 min. Subsequently, cells were incubated with FITC-lectin reagent (available in the kit) and then observed by fluorescence microscope (ZEISS, Germany).

Tumor Xenograft Experiments. A375 xenografts were produced on the back of 6-week-old female athymic nude-Foxn1$^{nu/nu}$ mice (Harlan, Italy) by subcutaneous injection of 5×10^6 A375 cells in 150 μL of Hanks' balanced salt solution. One week after tumor cell injection, mice with similar tumor sizes were randomized into three groups (10 mice per group) and treated with control PBS (100 μL), peptide **1** or **2** (200 nM), via intratumoral injection twice a week. Tumor size was measured once every week by caliper, and tumor volume was calculated according to the formula $V = (ab^2)/2$, (where a is the largest superficial diameter and b is the smallest superficial diameter). Animals were sacrificed when the tumor reached 1500 mm^3. Differences among the treatment groups were analyzed by ANOVA using statistical software (Statistica, StatSoft, Tulsa, OK). All animal experiments were performed in accordance with the European Communities Council Directive (86/609/EEC).

Immunohistochemistry. Tumors, excised after 1 week of treatments, were fixed overnight in neutral buffered formalin and processed by routine methods. For immunohistochemical analysis, 5 μm thick paraffin sections were deparaffinized and alcohol-rehydrated. Slides were treated with a 0.3% solution of hydrogen peroxidase in methanol to block the endogenous peroxidase activity for 30 min and then washed in phosphate buffer solution before immunoperoxidase staining.

The slides were then incubated for 1 h in a humidified chamber with the primary antibodies. Tissue sections were washed thoroughly with phosphate buffer solution and incubated with a biotinylated secondary antibody for 1 h, then rinsed and incubated with avidin−biotin peroxidase complex (ABC Kit, VectorLaboratories) for 1 h and developed with diaminobenzidine (Sigma) for 3 min. Sections were counterstained with hematoxylin. Finally, the slides were mounted with Permount. The antibody used in this analysis was an anti-CD31 (rat monoclonal antibody, Santa Cruz, CA, U.S.). Vessels were counted in 10 fields of the tumor section and referenced as number of blood vessels/field.

Statistical Analysis. Statistical analysis was performed using GraphPad Prism, version 4.00, for Windows, (GraphPad Software, www.graphpad.com). Results are reported as the mean with SD of at least four experiments run in three to five replicates, unless otherwise specified. Deviations from normal distribution were checked with the Shapiro−Wilk and Shapiro−Francia tests for normality. Comparisons between control and treated samples were made with a paired Student's *t* test.

Circular Dichroism Spectroscopy. CD spectra were collected at 20 °C in the range 260−190 nm by using 1 mm path-length quartz cuvette (Hellma, Milan, Italy) on a Jasco 720 instrument (Easton, MD, U.S.) using the following parameters: scanning speed 10 nm/min, bandwidth 2.0 nm, response 8 s, and three spectra accumulations. All experiments were performed in 10 mM phosphate buffer, pH 7.1, at a

peptide concentration of 60 μM. Peptide concentration was determined by absorbance at 280 nm. CD spectra were converted and displayed in mean residue ellipticity.

NMR Spectroscopy. NMR samples were prepared by dissolving 0.47 mg of the peptide in 500 μL of H_2O containing 10% ^2H_2O by volume at pH 6.5 (final peptide concentration, 0.5 mM). Two dimensional spectra, such as DQF-COSY,[35] TOCSY,[36] and NOESY[37] spectra, were recorded at 298 K on a Varian Inova 600 MHz spectrometer (Palo Alto, CA, U.S.), equipped with a cold probe. Water suppression was achieved through double pulsed field gradient spin echo sequences. For peptide **1**, mixing times of 70 ms for TOCSY and 250 ms for NOESY was applied. DQF-COSY spectra were acquired with 4096 data points in the direct dimension and 500 increments with 64 scans to obtain enough resolution to measure the $^3J_{HNH\alpha}$ coupling constants. Spectral processing was carried out using the software XwinNMR (Bruker AG, Billerica, MA, U.S.), and the spectra were analyzed with Neasy, a tool of computer aided resonance assignment (CARA) software.[38] Temperature dependence of the chemical shifts of the exchangeable amide protons was measured from TOCSY and 1D NMR spectra, recorded for at least five temperatures, 298, 301, 304, 307, and 310 K. The diffusion-ordered NMR spectroscopy (DOSY)[39,40] was carried out at 298 K using a 5 mm triple resonance *xyz* gradient probe head which delivers a maximum gradient strength of 50 G/cm on peptide **1**. The strength of the gradient pulses, of 3 ms duration, was incrementated in 16 experiments, with a diffusion time of 100 ms and a longitudinal eddy current delay of 5 ms. The water resonance was suppressed by low-power presaturation during the relaxation delay of 2 ms. The relationship between hydrodynamic radius (Rh) and diffusion coefficient (D) is given by the Stokes−Einstein equation: $Rh = kT/(6\pi\eta D)$ where k is the Boltzmann constant, T is the temperature (298 K), η is the viscosity of the solvent (0.91×10^{-3} for a mixture of 90% H_2O/10% D_2O), and D is the diffusion constant.

Structure calculation was performed with the software CYANA, version 2.1,[41] employing experimental distance restraints derived from the cross-peak intensities in NOESY spectra. Distance constraints together with 12 coupling constants for peptide **1** were then used to generate a set of allowable dihedral angles. Structure calculations were then started from 100 randomized conformers; the 20 conformers with the lowest CYANA target function were further refined by means of restrained energy minimization, using the Gromos 96 force field, with the program SPDB VIEWER.[42] The color figures and the structure analyses were performed with the program MOLMOL.[43]

Serum Stability Assays. The serum stabilities of peptides **1** and **2** were determined in 25% (v:v) aqueous pooled serum from human male AB plasma (Sigma, Milan, Italy). Peptides were dissolved in H_2O/CH_3CN (70:30 v:v), then diluted in serum at a final concentration of 0.5 mg/mL and incubated at 37 °C. Aliquots (20 μL) taken after 0, 15, 30, 60, 90, 120 min and 24 h were centrifuged at 4 °C. The supernatant was diluted with H_2O (0.1% TFA) at a final concentration of 0.1 mg/mL and stored at −20 °C. The samples were analyzed by RP-HPLC using a Phenomenex Jupiter C18 column (250 mm × 4.60 mm, 5 μm, 300 Å) and an isocratic elution at 38% of CH_3CN (0.1% TFA) for 10 min followed by a linear gradient from 38% to 48% of CH_3CN (0.1% TFA) in 5 min at a flow of 1 mL/min. The amount of intact peptide was estimated by integrating the area under the corresponding elution peak monitored at 210 nm.

■ ASSOCIATED CONTENT

Ⓢ Supporting Information. CD data, DOSY-NMR, chemical shift index, NOE pattern of peptide **1**, and serum stability assays. This material is available free of charge via the Internet at http://pubs.acs.org.

■ AUTHOR INFORMATION

Corresponding Author

*Phone: +39 081 2536679. Fax: +39 081 2534574. E-mail: ldandrea@unina.it.

Author Contributions

∞These authors contributed equally.

■ ACKNOWLEDGMENT

This work was supported by the DFM Scarl and MIUR (PRIN2008, No. 200875WHMR). We thank G. Perretta, L. Zona, and L. De Luca for technical assistance.

DEDICATION

†This paper is dedicated to the memory of Prof. Arturo Leone.

■ ABBREVIATIONS USED

AMC, 7-amino-4-methylcoumarin; AKT, RAC-α-serine/threonine-protein kinase; BME, basement membrane extract; DIPEA, *N*,*N*-diisopropylethylamine; DIVAA, directed in vivo angiogenesis assay; DMF, *N*,*N*-dimethylformamide; DOSY, diffusion-ordered spectroscopy; DQF, double-quantum filtered; DTT, dithiothreitol; EBM, endothelial cell basal medium; EC, endothelial cell; EDT, ethanedithiol; EDTA, ethylenediaminetetraacetic acid; ERK, extracellular-signal-regulated kinase; FITC, fluorescein isothiocyanate; GAPDH, glyceraldehyde 3 phosphate dehydrogenase; HATU, *N*,*N*,*N*′,*N*′-tetramethyl-*O*-(7-azabenzotriazol-1-yl)uronium hexafluorophosphate; HBTU, 2-(1*H*-benzotriazole-1-yl)-1,1,3,3-tetramethyluronium hexafluorophosphate; HEPES, 4-(2-hydroxyethyl)-1-piperazineethanesulfonic acid; HOBt, 1-hydroxybenzotriazole; HUVEC, human umbilical vein endothelial cell; mAb, monoclonal antibody; MBHA, 4-methylbenzhydrylamine; PE, phycoerythrin; RB, retinoblastoma protein; TFA, trifluoroacetic acid; TIS, triisopropylsilane; TOCSY, total correlation spectroscopy; VEGF, vascular endothelial growth factor; VEGFR, vascular endothelial growth factor receptor

■ REFERENCES

(1) Carmeliet, P. Angiogenesis in life, disease and medicine. *Nature* **2005**, *438*, 932–936.

(2) Folkman, J. Angiogenesis. *Annu. Rev. Med.* **2006**, *57*, 1–18.

(3) Molin, D.; Post, M. J. Therapeutic angiogenesis in the heart: protect and serve. *Curr. Opin. Pharmacol.* **2007**, *7*, 158–163.

(4) Ferrara, N.; Gerber, H. P.; LeCouter, J. The biology of VEGF and its receptors. *Nat. Med.* **2003**, *9*, 669–676.

(5) Greenberg, D. A.; Jin, K. From angiogenesis to neuropathology. *Nature* **2005**, *438*, 954–959.

(6) Olsson, A. K.; Dimberg, A.; Kreuger, J.; Claesson-Welsh, L. VEGF receptor signalling: in control of vascular function. *Nat. Rev. Mol. Cell Biol.* **2006**, *7*, 359–371.

(7) Autiero, M.; Waltenberger, J.; Communi, D.; Kranz, A.; Moons, L.; Lambrechts, D.; Kroll, J.; Plaisance, S.; De Mol, M.; Bono, F.; Kliche, S.; Fellbrich, G.; Ballmer-Hofer, K.; Maglione, D.; Mayr-Beyrle, U.; Dewerchin, M.; Dombrowski, S.; Stanimirovic, D.; Van Hummelen, P.; Dehio, C.; Hicklin, D. J.; Persico, G.; Herbert, J. M.; Communi, D.; Shibuya, M.; Collen, D.; Conway, E. M.; Carmeliet, P. Role of PlGF in the intra- and intermolecular cross talk between the VEGF receptors Flt1 and Flk1. *Nat. Med.* **2003**, *9*, 936–943.

(8) Fischer, C.; Mazzone, M.; Jonckx, B.; Carmeliet, P. FLT1 and its ligands VEGFB and PlGF: drug targets for anti-angiogenic therapy? *Nat. Rev. Cancer* **2008**, *8*, 942–56.

(9) Nagy, J. A.; Dvorak, A. M.; Dvorak, H. F. VEGF-A and the induction of pathological angiogenesis. *Annu. Rev. Pathol.: Mech. Dis.* **2007**, *2*, 251–275.

(10) D'Andrea, L. D.; Iaccarino, G.; Fattorusso, R.; Sorriento, D.; Carannante, C.; Capasso, D.; Trimarco, B.; Pedone, C. Targeting angiogenesis: structural characterization and biological properties of a de novo engineered VEGF mimicking peptide. *Proc. Natl. Acad. Sci. U.S. A.* **2005**, *102*, 14215–14220.

(11) Wiesmann, C.; Fuh, G.; Christinger, H. W.; Eigenbrot, C.; Wells, J. A.; de Vos, A. M. Crystal structure at 1.7 Å resolution of VEGF in complex with domain 2 of the Flt-1 receptor. *Cell* **1997**, *91*, 695–704.

(12) Pedram, A.; Razandi, M.; Levin, E. R. Extracellular signal-regulated protein kinase/Jun kinase cross-talk underlies vascular endothelial cell growth factor-induced endothelial cell proliferation. *J. Biol. Chem.* **1998**, *273*, 26722–26728.

(13) Fujio, Y.; Walsh, K. Akt mediates cytoprotection of endothelial cells by vascular endothelial growth factor in an anchorage-dependent manner. *J. Biol. Chem.* **1999**, *274*, 16349–16354.

(14) Yilmaz, A.; Kliche, S.; Mayr-Beyrle, U.; Fellbrich, G.; Waltenberger, J. p38 MAPK inhibition is critically involved in VEGFR-2-mediated endothelial cell survival. *Biochem. Biophys. Res. Commun.* **2003**, *306*, 730–736.

(15) Steensma, D. P.; Timm, M.; Witzig, T. E. Flow cytometric methods for detection and quantification of apoptosis. *Methods Mol. Med.* **2003**, *85*, 323–332.

(16) Conway, E. M.; Collen, D.; Carmeliet, P. Molecular mechanisms of blood vessel growth. *Cardiovasc. Res.* **2001**, *49*, 507–521.

(17) Ferrara, N. Role of vascular endothelial growth factor in regulation of physiological angiogenesis. *Am. J. Physiol.: Cell Physiol.* **2001**, *280*, C1358–C1366.

(18) Yao, S.; Howlett, G. J.; Norton, R. S. Peptide self-association in aqueous trifluoroethanol monitored by pulsed field gradient NMR diffusion measurements. *J. Biomol. NMR* **2000**, *16*, 109–119.

(19) Diana, D.; Ziaco, B.; Colombo, G.; Scarabelli, G.; Romanelli, A.; Pedone, C.; Fattorusso, R.; D'Andrea, L. D. Structural determinants of the unusual helix stability of a de novo engineered vascular endothelial growth factor (VEGF) mimicking peptide. *Chem.—Eur. J.* **2008**, *14*, 4164–4166.

(20) Diana, D.; Ziaco, B.; Scarabelli, G.; Pedone, C.; Colombo, G.; D'Andrea, L. D.; Fattorusso, R. Structural analysis of a helical peptide unfolding pathway. *Chem.—Eur. J.* **2010**, *16*, 5400–5407.

(21) Wüthrich, K. *NMR of Proteins and Nucleic Acids*; Wiley: New York, 1986.

(22) Wishart, D. S.; Sykes, B. D.; Richards, F. M. The chemical shift index: a fast and simple method for the assignment of protein secondary structure through NMR spectroscopy. *Biochemistry* **1992**, *31*, 1647–1651.

(23) D'Andrea, L. D.; Del Gatto, A.; Pedone, C.; Benedetti, E. Peptide-based molecules in angiogenesis. *Chem. Biol. Drug Des.* **2006**, *67*, 115–126.

(24) D'Andrea, L. D.; Del Gatto, A.; De Rosa, L.; Romanelli, A.; Pedone, C. Peptides targeting angiogenesis related growth factor receptors. *Curr. Pharm. Des.* **2009**, *15*, 2414–2429.

(25) Zilberberg, L.; Shinkaruk, S.; Lequin, O.; Rousseau, B.; Hagedorn, M.; Costa, F.; Caronzolo, D.; Balke, M.; Canron, X.; Convert, O.; Laïn, G.; Gionnet, K.; Goncalvès, M.; Bayle, M.; Bello, L.; Chassaing, G.; Deleris, G.; Bikfalvi, A. Structure and inhibitory effects on angiogenesis and tumor development of a new vascular endothelial growth inhibitor. *J. Biol. Chem.* **2003**, *278*, 35564–35573.

(26) Goncalves, V.; Gautier, B.; Coric, P.; Bouaziz, S.; Lenoir, C.; Garbay, C.; Vidal, M.; Inguimbert, N. Rational design, structure, and biological evaluation of cyclic peptides mimicking the vascular endothelial growth factor. *J. Med. Chem.* **2007**, *50*, 5135–5146.

(27) Gautier, B.; Goncalves, V.; Diana, D.; Di Stasi, R.; Teillet, F.; Lenoir, C.; Huguenot, F.; Garbay, C.; Fattorusso, R.; D'Andrea, L. D.; Vidal, M.; Inguimbert, N. Biochemical and structural analysis of the binding determinants of a vascular endothelial growth factor receptor peptidic antagonist. *J. Med. Chem.* **2010**, *53*, 4428–4440.

(28) Mirassou, Y.; Santiveri, C. M.; Perez de Vega, M. J.; Gonzalez-Muniz, R.; Jimenez, M. A. Disulfide bonds versus TrpTrp pairs in irregular beta-hairpins: NMR structure of vammin loop 3-derived peptides as a case study. *ChemBioChem* **2009**, *10*, 902–910.

(29) Takahashi, T.; Yamaguchi, S.; Chida, K.; Shibuya, M. A single autophosphorylation site on KDR/Flk-1 is essential for VEGF-A-dependent activation of PLC-gamma and DNA synthesis in vascular endothelial cells. *EMBO J.* **2001**, *20*, 2768–2678.

(30) Dudar, G. K.; D'Andrea, L. D.; Di Stasi, R.; Pedone, C.; Wallace, J. L. A vascular endothelial growth factor mimetic accelerates gastric ulcer healing in an iNOS-dependent manner. *Am. J. Physiol.: Gastrointest. Liver Physiol.* **2008**, *295*, G374–G381.

(31) Santulli, G.; Ciccarelli, M.; Palumbo, G.; Campanile, A.; Galasso, G.; Ziaco, B.; Altobelli, G. G.; Cimini, V.; Piscione, F.; D'Andrea, L. D.; Pedone, C.; Trimarco, B.; Iaccarino, G. In vivo properties of the proangiogenic peptide QK. *J. Transl. Med.* **2009**, *7*, 41–50.

(32) Livnah, O.; Johnson, D. L.; Stura, E. A.; Farrell, F. X.; Barbone, F. P.; You, Y.; Liu, K. D.; Goldsmith, M. A.; He, W.; Krause, C. D.; Pestka, S.; Jolliffe, L. K.; Wilson, I. A. An antagonist peptide-EPO receptor complex suggests that receptor dimerization is not sufficient for activation. *Nat. Struct. Biol.* **1998**, *5*, 993–1004.

(33) Chan, W. C.; White, P. D. *Fmoc Solid Phase Peptide Synthesis*; Oxford University Press: Oxford, U.K., 2000; pp 303−327.

(34) Thornberry, N. A.; Bull, H. G.; Calaycay, J. R.; Chapman, K. T.; Howard, A. D.; Kostura, M. J.; Miller, D. K.; Molineaux, S. M.; Weidner, J. R.; Aunins, J.; Elliston, K. O.; Ayala, J. M.; Casano, F. J.; Chin, J.; Ding, G. J.-F.; Egger, L. A.; Gaffney, E. P.; Oksana, G. L.; Palyha, C.; Raju, S. M.; Rolando, A. M.; Salley, J. P.; Yamin, T. T.; Lee, T. D.; Shively, J. E.; MacCross, M.; Mumford, R. A.; Schmidt, J. A.; Tocci, M. J. A novel heterodimeric cysteine protease is required for interleukin-1 beta processing in monocytes. *Nature* **1992**, *356*, 768–774.

(35) Rance, M.; Sorensen, O. W.; Bodenhausen, G.; Wagner, G.; Ernst, R. R.; Wüthrich, K. Improved spectral resolution in cosy ^{1}H NMR spectra of proteins via double quantum filtering. *Biochem. Biophys. Res. Commun.* **1983**, *117*, 479–485.

(36) Griesinger, C.; Otting, G.; Wüthrich, K.; Ernst, R. R. Clean TOCSY for ^{1}H spin system identification in macromolecules. *J. Am. Chem. Soc.* **1988**, *110*, 7870–7872.

(37) Kumar, A.; Ernst, R. R.; Wüthrich, K. A two-dimensional nuclear Overhauser enhancement (2D NOE) experiment for the elucidation of complete proton−proton cross-relaxation networks in biological macromolecules. *Biochem. Biophys. Res. Commun.* **1980**, *95*, 1–6.

(38) Masse, J. M.; Keller, R. AutoLink: automated sequential resonance assignment of biopolymers from NMR data by relative-hypothesis-prioritization-based simulated logic. *J. Magn. Reson.* **2005**, *174*, 133–151.

(39) Morris, K. F.; Johnson, J. C. S. Diffusion-ordered two-dimensional nuclear magnetic resonance spectroscopy. *J. Am. Chem. Soc.* **1992**, *114*, 3139–3141.

(40) Johnson, J. C. S. Diffusion ordered nuclear magnetic resonance spectroscopy: principles, applications. *Prog. Nucl. Magn. Reson. Spectrosc.* **1999**, *34*, 203–256.

(41) Herrmann, T.; Güntert, P.; Wüthrich, K. Protein NMR structure determination with automated NOE assignment using the new software CANDID and the torsion angle dynamics algorithm DYANA *J. Mol. Biol.* **2002**, *319*, 209–227.

(42) Guex, N.; Peitsch, M. C. SWISS-MODEL and the Swiss-PdbViewer: an environment for comparative protein modelling. *Electrophoresis* **1997**, *18*, 2714–2723.

(43) Koradi, R.; Billeter, M.; Wüthrich, K. MOLMOL: a program for display and analysis of macromolecular structures. *J. Mol. Graphics* **1996**, *14*, 29–32.